



Published in final edited form as:

Traffic. 2014 January ; 15(1): . doi:10.1111/tra.12132.

Disruption of clathrin-mediated trafficking causes centrosome overduplication and senescence

Maciej B. Olszewski^{1,2}, Panagiotis Chandris¹, Bum-Chan Park¹, Evan Eisenberg¹, and Lois E. Greene^{1,2}

¹ Laboratory of Cell Biology, National Heart Lung and Blood Institute, National Institutes of Health

Abstract

The Hsc70 cochaperone, G cyclin-associated kinase (GAK), has been shown to be essential for the chaperoning of clathrin by Hsc70 in the cell. In this study, we used conditional GAK knockout mouse embryonic fibroblasts (MEFs) to determine the effect of completely inhibiting clathrin-dependent trafficking on the cell cycle. After GAK was knocked out, the cells developed the unusual phenotype of having multiple centrosomes, but at the same time failed to divide and ultimately became senescent. To explain this phenotype, we examined the signaling profile and found that mitogenic stimulation of the GAK KO cells and the control cells were similar except for increased phosphorylation of Akt. In addition, the disruption of intracellular trafficking caused by knocking out GAK destabilized the lysosomal membranes, resulting in DNA damage due to iron leakage. Knocking down clathrin heavy chain or inhibiting dynamin largely reproduced the GAK KO phenotype, but inhibiting only clathrin-mediated endocytosis by knocking down AP2 caused growth arrest and centrosome overduplication, but no DNA damage or senescence. We conclude that disruption of clathrin-dependent trafficking induces senescence accompanied by centrosome overduplication because of a combination of DNA damage and changes in mitogenic signaling that uncouples centrosomal duplication from DNA replication.

Keywords

Endocytosis; trafficking; senescence; centrosome; overduplication; DNA damage; clathrin

Introduction

Cell cycle progression is dependent on mitogenic factors such as epidermal growth factor (EGF) or platelet derived growth factor (PDGF) binding to their respective receptors on the plasma membrane. This in turn activates signal-transducing cascades that ultimately initiate DNA synthesis. Even though signaling starts when the mitogens bind to their receptors, it persists after internalization. As the receptors traffic along the endocytic pathway, the composition of the signaling complexes changes, which significantly alters the biological output of the signal (1-4). The signaling cascade is also affected by whether the receptor is internalized via clathrin-mediated endocytosis (CME) or clathrin-independent endocytosis. Since the pathway of internalization often defines the final outcome of the signaling event (5), it is important to understand how blocking clathrin-dependent trafficking affects cell cycle progression.

The effect of inhibiting CME on cell cycle progression has been examined by several laboratories, but there is still controversy as to the cellular phenotype that develops. When

² To whom correspondence should be addressed at molszewski@iimcb.gov.pl or greenel@helix.nih.gov.

CME was blocked by knocking down either clathrin or AP2 by RNA interference, the growth arrested HeLa cells did not initiate DNA replication when stimulated by EGF (5). This shows that CME is necessary for EGF signaling to induce progression of cells through the G1 restriction point. This, in turn, would predict that knocking-down clathrin would inhibit cells from reaching mitosis. However, knocking-down clathrin in NRK and HEK293 cells caused a 4-fold increase in mitotic cells, which was in part due to prolonged mitosis caused by chromosome misalignment stemming from defective congression of chromosomes (6). An increase in mitotic cells was also observed when CME was blocked in HeLa cells by knocking down GAK (7), an Hsc70-cochaperone that is required for clathrin uncoating and clathrin chaperoning in the cytosol (8-10). Another unexpected phenotype that was observed in the GAK-depleted HeLa cells was that the centrosomes became fragmented (7). A similar phenotype has recently been reported in clathrin-depleted HeLa cells (11), but has not been observed in NRK cells (6). Interestingly, even though the cell cycle is profoundly altered by inhibiting CME, inhibition of CME by knocking out dynamin in MEFs does not significantly affect Akt and ERK mitogenic signaling stimulated by EGF (12). Similarly, pharmacological dynamin inhibition prevents the proliferative response of human fibroblasts to PDGF without affecting these major signal transduction pathways (13).

To better understand the effect of inhibiting clathrin trafficking on the cell cycle, we utilized mouse embryonic fibroblasts (MEFs) derived from a GAK conditional knockout mouse, engineered in our laboratory (14). Our previous studies showed that when GAK is depleted, CME is inhibited and trafficking of clathrin-dependent cargo from the trans-Golgi network (TGN) is markedly altered (10, 15, 16). In addition, there is a loss of both clathrin-coated pits from the plasma membrane and perinuclear clathrin associated with the TGN. The key advantage of the conditional knockout-based system over traditional siRNA-based knockdown is that GAK depletion is complete, which is critical since this protein acts catalytically and minimal amounts are sufficient to support clathrin-dependent trafficking.

We now report that inhibiting clathrin-dependent trafficking by knocking out GAK, knocking down AP2 or CHC or inhibiting dynamin with dynasore results in growth arrest, cessation of DNA synthesis and overduplication of centrosomes. With all of the above treatments except for the AP2 KD, there was DNA damage, which was caused by iron leakage from the lysosome. This produced a low level of genotoxic stress, which when accompanied by altered mitogenic stimulation, eventually led to the development of senescence. These results show that disruption of clathrin-dependent trafficking in MEFs uncouples centrosome duplication from DNA synthesis and leads to the development of an unusual phenotype combining senescence with centrosome overduplication.

Results

GAK depletion causes disruption of clathrin function and growth arrest

In order to knock out GAK, mouse embryonic fibroblasts (MEFs) obtained from GAK/flox mouse (10) were infected with Cre-encoding adenovirus (AdCre). Control and GAK KO cells were seeded on coverslips 4 days post-infection and on day 6 post-infection the cells were fixed and stained for clathrin heavy chain and AP-2, a clathrin adapter protein (Fig. 1A). In control cells, clathrin is organized on the plasma membrane as coated pits, which contains AP-2. In contrast, in GAK KO cells organization of both clathrin and AP-2 is disrupted; clathrin is localized in small clusters scattered throughout cytoplasm that are negative for AP-2, while AP-2 is predominantly clustered along the cell periphery. This shows that the loss of GAK prevents formation of functional clathrin-coated pits, which results in inhibition of CME (10). Not only is clathrin localization disrupted by the absence of clathrin, but clathrin exchange between cytoplasmic and pit-assembled pools is markedly inhibited in GAK KO cells. The efficiency of this process was analyzed by fluorescence

recovery after photobleaching (FRAP) in control and GAK KO cells transfected with clathrin light chain (LCa) GFP fusion protein (Fig. 1B). Fluorescent vesicular structures localized at the base of the cell were photobleached and fluorescence recovery was monitored. In control cells 85% of fluorescence recovered within 4 min indicating that the bleached clathrin mostly exchanged with the fluorescent cytoplasmic clathrin. In contrast, in GAK KO cells only 20% of fluorescence recovered during the same time indicating that the process of clathrin exchange is impaired in the absence of GAK. Therefore, in agreement with our previous results, in the absence of GAK, Hsc70 no longer chaperones clathrin, which in turn inhibits clathrin-dependent trafficking in the cell.

Having established that in GAK KO MEFs clathrin function is disrupted, these cells were used to study the effect of inhibiting clathrin trafficking on the cell cycle. Monitoring the density of the GAK KO MEFs showed that knocking out GAK profoundly affected cell growth; the cells stopped growing. To quantify this phenotype, the cells were plated three days post-infection and the density of infected and non-infected cultures was monitored by methylene blue staining (17). Non-infected cells grew to confluency, while cells infected with AdCre showed only limited growth and subsequently ceased to divide (Fig. 1C). When DNA replication was assayed by examining EdU incorporation in a pulse-label experiment, there was a steady decrease in EdU incorporation following adenovirus infection (Fig. 1D and 1E). When compared to the control MEFs, the population of mitotic cells in the GAK KO MEFs was decreased, as assessed by the decreased number of cells showing Ser28 histone H3 phosphorylation (Fig. 1E). DNA content analysis by FACS showed that the 2N and 4N populations in GAK KO cells were similar to these observed in control MEFs but the fraction of S-phase cells was decreased (Fig. 1F). This indicates that the initial growth arrest does not occur at any specific stage of the cell cycle, but rather at multiple checkpoints. Thus GAK depletion not only prevents G1 cells from entering S phase, but also interferes with the entry of the G2 cells into mitosis, resulting in a stable population of tetraploid cells.

GAK KO causes senescence and centrosome overduplication

Prolonged growth arrest either results in cell death or leads to a stable state of quiescence or senescence. Since GAK KO cells remained viable for several weeks after AdCre infection, we examined whether they had become senescent by staining for β -galactosidase, an established marker of senescence (18, 19). As shown in Fig. 2A, after 10 or more days in culture, unlike the control cells, the GAK KO cells exhibited blue staining characteristic of senescent cells. To confirm that the GAK KO cells had irreversibly lost their proliferative potential, as opposed to the reversible growth arrest found in quiescent cells, an in vitro DNA replication assay was performed by harvesting nuclei and cytosol from control and GAK KO cells (20). Control cytosol was harvested from cells that were synchronized at the beginning of S phase, while nuclei were harvested from non-synchronized cultures. As shown in Fig. 2B, control nuclei incubated in the presence of S-phase cytosol derived from control cells synthesized DNA efficiently. On the other hand, nuclei from GAK KO cells did not resume DNA synthesis when incubated with S-phase cytosol derived from control cells. This indicates that the GAK KO nuclei lost their proliferative potential, a phenotype characteristic of senescent cells. However, the control nuclei incubated with cytosol derived from GAK KO cells exhibited markedly lower but still significant DNA synthesis. This suggests that the loss of nuclear proliferative potential in GAK KO cells (senescence) is intrinsic to the nucleus. The fact that the cytosol of GAK KO cells supports limited DNA replication in control nuclei indicates that the mitogenic signaling in the GAK KO cytosol is sufficient to induce DNA synthesis.

During cell cycle progression centrosomes duplicate in parallel to DNA synthesis. Since the GAK KO cytosol retained mitogenic activity and fragmented centrosomes have in fact been

observed following GAK or CHC knockdown (6, 7), we examined the number and integrity of centrosomes by staining for centrin and γ -tubulin. Microscopic analysis revealed that the number of centrosomes per GAK KO cell reached values as high as 15; these centrosomes were positive for both centrin and γ -tubulin (Fig 2C, D), indicating uncontrolled centriolar duplication and maturation rather than centrosome fragmentation due to structural instability, as reported previously (7). Quantitation of the percent of cells with abnormal centrosome numbers (3 or more) showed that more than 60% of the GAK KO cells had multiple centrosomes, as compared to ca. 3% of the control cells (Fig. 2E).

To determine the cause of this centrosome overduplication, we first examined whether the loss of p53 activity was responsible for this phenotype; loss of p53 activity could have occurred when the MEFs became spontaneously immortalized. This was tested by culturing the GAK KO MEFs in 2 mM hydroxyurea (HU) for 48h (21), which would produce centrosome overduplication if the MEFs were deficient in p53 activity. Following HU treatment, the cells were stained for γ -tubulin and the centrosomes were counted. HU-treated cells did not exhibit increased numbers of centrosomes as compared to non-treated cells (Fig. 2E), indicating that DNA synthesis and centrosome duplication are coupled in the presence of GAK and uncoupling only occurs after GAK depletion. We also examined by immunostaining whether Plk4 was present on the centrosomes in the GAK KO cells. Plk4 is a major regulator of centriole duplication (22) and its overexpression alone can induce the overduplication phenotype (23, 24). Cells were grown on coverslips, fixed, stained for γ -tubulin and Plk4, and imaged on a confocal microscope. Control cells with one centrosome (G1 cells) showed Plk4 localization at the centrosome (Fig. 2F), whereas control cells with two distant centrosomes (late S or G2) exhibited low levels or no colocalization of Plk4 and γ -tubulin (Fig. 2G). In contrast, Plk4 was found on the overduplicated centrosomes in the GAK KO cells (Fig. 2H), indicating that Plk4 activity might be involved in the mechanism of GAK KO-induced centrosome overduplication (24).

Signaling Profile of GAK KO cells is consistent with senescence

Since the nuclei from the GAK KO cells showed irreversible loss of proliferative potential, there should be alterations in the regulatory pathways associated with cell cycle progression that caused this phenotype. The Western blot analysis in Fig.3 compares the levels of a selection of important cell cycle regulators in lysates from control, GAK KO, and quiescent (serum-starved) MEFs. The GAK KO cells, but not the control cells and quiescent cells, showed increases in phosphorylation of p53 on Ser15 and the level of p21. Both sustained p53 activation and p21 level may lead to the development of senescence (25, 26)

To determine which kinase was responsible for the p53 activation, we tested several kinase inhibitors. Inhibiting ATM kinase with 20 μ M KU55933 reduced the level of Ser15 phospho-p53 to control level (Fig. 3B), which shows that p53 is phosphorylated by ATM. Inhibition of p38 with SB203580 did not reduce the phosphorylation of p53. Therefore, the senescence pathway in GAK KO cells involves phosphorylation of p53 by ATM, which in turn upregulates p21. This causes inhibition of CDK2 and consequently growth arrest. Unlike the GAK KO MEFs, the growth arrest in quiescent cells appears to be due to up regulation of the CDK inhibitors, p16 and p27.

Surprisingly, the activating Thr160 residue in CDK2 is phosphorylated to the same extent in the control and the GAK KO MEFs. Typically, this residue is not phosphorylated in senescent and quiescent cells (27). In addition, the level of cyclin E is similar in GAK KO MEFs and control cells, while it is much lower in quiescent cells. Cyclin E interacts with CDK2 to regulate G1/S transition and centrosome duplication (28). Cyclin D1 is upregulated in GAK KO MEFs, but not in control and quiescent MEFs, which is typical for cells undergoing senescence (29). In addition, cyclin A and cyclin B1 levels are much lower in

GAK KO MEFs and quiescent cells than in control cells. Cyclin A and Cyclin B1 regulate cell cycle progression through S, G2 and mitosis. Therefore, the GAK KO MEFs containing 4N DNA are not G2 cells but are cells that were arrested at G2/M or spindle checkpoints and, unable to enter or complete mitosis, have exited the cell cycle.

CDK2 activity suppresses cellular senescence (30, 31) and one of the most potent CDK2 inhibitors that is also known to induce senescence is p21 (26, 29). Considering that GAK KO cells become senescent and p21 level is elevated in these cells, we examined whether more p21 was bound to CDK2 in the GAK KO cells than in control cells. Immunoprecipitating CDK2 showed that much more p21 coimmunoprecipitated in the GAK KO MEFs than in the control cells (Fig. S1A). Next, we measured whether the CDK2 complexes had lower specific kinase activity in GAK KO lysates than in control lysates by using histone H1 and [³²P]ATP as substrates. Autoradiograph of the histone H1-associated radioactivity showed lower specific kinase activity of CDK2 complexes immunoprecipitated from GAK KO lysates than from control lysates. (Fig. S1B). Therefore, the inhibitory p53/p21 pathway is activated in the GAK KO cells, which results in net CDK2 activity decrease, thereby facilitating the onset of senescence. In summary, given the normal levels of activatory Thr160 CDK2 and Tyr202/204 ERK phosphorylations, the signaling profile is indicative of conflicting mitogenic and genotoxic stimuli, which leads to cell senescence (26, 32).

Lysosomal membrane instability in GAK KO cells leads to iron leak and DNA damage

Since the markers of an ongoing DNA damage response were found in the GAK KO cells, microscopic analysis of this phenotype was performed in control and GAK KO cells by staining for Ser15 phospho-p53 and Ser1981 phospho-ATM, that both associate with DNA breaks (33, 34). Compared to control cells, the GAK KO cells had more numerous and more intense foci positive for both phospho-p53 and phospho-ATM, indicating an increased number of DNA breaks in these cells (Fig. 4A and B, respectively). Among the many agents capable of damaging the DNA, one are the non-chelated iron ions that, while redox cycling, generate free radicals that may damage the DNA (35-37). When lysosomal homeostasis is disturbed, redox-active iron may be released from lysosomes and upon reaching the nuclear compartment may damage the DNA (38). Interestingly, the trafficking of cargo from the TGN to the lysosome is disrupted in the GAK KO cells (16), which raises the possibility that a defect in the stability of the lysosomal membrane results in the release of iron into the cytosol.

To determine whether lysosomal membranes are destabilized in the GAK KO cells, both control and GAK KO MEFs were allowed to internalize acridine orange to label the lysosomal compartment. Subsequently, the cells were imaged under low-intensity 488 nm excitation light to induce acridine orange-mediated lysosomal membrane disruption to measure of lysosomal membrane stability (39). Sufficient exposure to blue light caused disruption of lysosomes in both control and GAK KO cells (Fig. 4C), but this disruption occurred much more readily in the GAK KO cells (Fig. 4D, whole image sequence available as supplementary movie 1), confirming that the lysosomal membranes are more unstable in the GAK KO cells.

We next examined whether the DNA damage in the GAK KO cells is caused by the release of iron into the cytosol. Control and GAK KO cells were cultured with an iron chelator, 0.2 mM desferrioxamine (DFX) for 12 h, beginning at day 6 post-KO, followed by staining for Ser15 phospho-p53 and Ser1981 phospho-ATM. The intensity and pattern of fluorescence in the DFX-treated control cells did not change when compared to non-treated cells (Fig. 4E and 4A, respectively). In contrast, DFX treatment of the GAK KO cells resulted in a marked decrease of both fluorescence intensity and foci number when compared to the non-treated

cells (Fig. 4F and 4B, respectively), indicating that the DNA breaks in these cells are caused by a labile (non-chelated) iron pool. The number of foci positive for phospho-p53 and phospho-ATM per nucleus was quantified and the results are shown in Fig. 4G. These data collectively indicate that knocking out GAK destabilizes lysosomal membranes, leading to iron leakage and DNA damage that in turn induces ATM-mediated p53 phosphorylation, leading to an increase in p21 level, which ultimately induces senescence in cells concurrently subjected to mitogenic stimulation (26).

Disrupted endocytosis causes centrosome overduplication while concomitant persistent DNA damage leads to senescence

Knocking out GAK causes at least two broadly defined phenotypes: centrosome overduplication and senescence. With regard to the latter phenotype, the inhibition of intracellular clathrin-dependent trafficking, perhaps at the TGN, apparently causes destabilization of the lysosomal membrane, leading to the release of iron and DNA damage. This led us to hypothesize that MEFs should not become senescent by inhibiting only CME, whereas exposing MEFs to low concentrations of a DNA damaging agent should cause senescence. To block CME, the α -adaptin subunit of the clathrin adaptor, AP2, was knocked down by using lentivirus encoding shRNA directed against α -adaptin. The cells were infected twice, 48 h apart and for the subsequent 4 days selected with puromycin to remove non-infected cells at which time the cells were analyzed. The efficiency of the knockdown was confirmed by Western blotting (Fig. 5A). Importantly, knocking down AP2 does not increase Ser15 phosphorylation of p53 which shows that the DNA damage observed in GAK KO cells is not caused by inhibition of CME. Alternatively, when the cells were exposed to low concentrations of a DNA-damaging agent camptothecin (CPT), their level of Ser 15 phospho-p53 was comparable to that of the GAK KO MEFs.

First, we examined the DNA synthesis in the control, DNA-damaged and AP2 KD cells by measuring EdU incorporation using FACs. In contrast to the control population, neither the DNA-damaged nor the AP2 KD cells showed significant EdU incorporation (Fig. 5B), showing that damaging DNA or inhibiting CME prevented DNA replication. This was confirmed by staining for Ki67 protein, a marker for proliferating cells. The percentage of cells positive for Ki67 decreased from 84% in control MEFs to 21% and 15% in DNA-damaged and AP2 KD cells, respectively, indicating that these treatments cause the cells to leave the cell cycle (Fig. 5C). Next, the DNA content of these different populations of cells was measured by FACS (Fig. 5D). When compared to control MEFs the AP2 KD cells mainly showed depletion of S-phase and 4N cells, while the DNA-damaged cells showed a significant accumulation of 4N cells. This suggests that inhibiting CME predominantly arrests the cells in G1 phase while damaging DNA primarily activates the G2/M checkpoint. In GAK KO cells depletion of S-phase cells was observed, with proportions of 2N and 4N cells reminiscent of the control cells. Western blot analysis (Fig. 5A) showed that the cyclins typical of the S and G2 phases (cyclins A and B1) are depleted in AP2 KD cells, as well as in the GAK KO cells, while there is a significant accumulation of these cyclins in DNA-damaged cells. In contrast, cyclin E, which normally reaches its highest level in late G1 phase, is slightly enriched in the GAK KO and AP2 KD cells but depleted in the DNA-damaged cells.

Since the two major phenotypes of the GAK KO cells were senescence and centrosome overduplication, we tested whether the AP2 KD or the DNA-damaged cells would show these phenotypes. To test for senescence, AP2 KD cells were fixed 10 days after the initial infection, while the DNA-damaged cells were exposed to 2 μ M CPT for 3 h daily for 6 days. As expected, given the lack of DNA damage in the AP2 KD cells, they did not exhibit β -galactosidase staining, a marker of senescence, whereas the DNA-damaged cells were positive for this marker (Fig. 5F). However, when we examined whether there was

overduplication of centrosomes by staining for γ -tubulin (Fig. 5E), 29% of the AP2 KD cells exhibited overduplicated centrosomes, whereas the DNA-damaged cells did not show any increase in the percentage of cells with overduplicated centrosomes. The extent of centrosome overduplication in the AP2 KD cells was lower than in the GAK KO cells (Fig. 2E), which may be caused by the different rates of GAK and AP2 loss in AdCre and shRNA treated cells, respectively. Alternatively, the higher prevalence of centrosome overduplication in the GAK KO cells compared to the AP2 KD cells may result from the loss of CME-independent functions in the GAK KO cells. In any event, these results show that the DNA damage contributes to the senescent phenotype, whereas blocking CME contributes to the overduplication of centrosomes.

Growth factor signaling required for centrosome overduplication in GAK KO cells is transduced by multiple kinases

Interestingly, even though DNA duplication is blocked in GAK KO and AP2 KD cells, these cells have overduplicated centrosomes. Centrosome duplication is one of the elements constituting normal cell cycle and therefore it might be expected to depend on mitogenic signaling. In order to verify that centrosome overduplication in GAK KO cells is dependent on the CME-independent mitogenic signaling, MEFs were infected with AdCre and beginning on day 3 post-KO cultured in medium containing 0.1% or 10% FBS for the next 3 days. A sample from the cells cultured in 0.1% FBS was fixed for immunofluorescence at 24 h (4 days post AdCre-infection), while the remaining cells were cultured for additional 48 h in 0.1% FBS with or without 100 ng/ml EGF. Graphic depiction of this experimental scheme is presented in Fig. 6A. The percentage of cells with overduplicated centrosomes was 3% and 68% after 6 days in medium with 10% FBS in control and GAK KO MEFs, respectively. In the population fixed on day 4 post-KO this percentage was 35% and in cells cultured for another 48 h in 0.1% FBS, the percentage was 29%. This decrease was not statistically significant and may be due to an increase in mortality in the population of KO cells with the lowest GAK level under low-serum conditions. In contrast, 52% of GAK KO cells cultured for 48 h in the 0.1% FBS medium supplemented with 100 ng/ml EGF had overduplicated centrosomes. These results show that stimulation with EGF alone is approximately 50% as efficient in inducing centrosome overduplication as with 10% FBS (Fig. 6B).

We also examined the mitogenic signaling necessary for centrosome overduplication by using kinase-specific inhibitors. The following kinase inhibitors and combinations thereof were added 4 days following GAK KO to the culture medium containing 10% FBS: roscovitine, UO126, AktVIII or SB203580 (inhibitors of CDK2, MEK, Akt and p38 MAP kinases, respectively). On day 6 post-KO cells were fixed and stained for γ -tubulin. Centrosomes were counted and the data are presented in Fig. 6C and D. All of the inhibitors decreased the prevalence of the overduplication phenotype in a statistically significant manner. Interestingly, while the inhibitor most effective in prevention of centrosome overduplication targets Akt kinase, in GAK KO and AP2 KD cells that both overduplicate their centrosomes the level of activatory Ser473 Akt phosphorylation is markedly increased when compared to control cells (Fig. 5A). When the inhibitors were used in pairs, the percentage of cells with overduplicated centrosomes was further decreased, as compared to single-inhibitor treatments. In fact, treatments with combined inhibitors prevented any statistically significant increase in the percentage of cells exhibiting the overduplication phenotype (Fig. 6D). The fact that the extent of inhibition of centrosome overduplication varied amongst the inhibitors suggested variable roles played by CDK2, MEK, Akt and p38 kinases in mitogenic signal transduction resulting in this phenotype. Our data showing that complete prevention of centrosome overduplication required treating the cells with

combinations of inhibitors suggests that multiple kinases concurrently contribute to centrosome overduplication.

In order to better characterize the activation state of several kinases that are involved in mitogenic signal transduction, lysates prepared from control and GAK KO MEF cells were analyzed by Western blotting. Fig. 6E shows that disruption of clathrin-mediated trafficking did not reduce the phosphorylation (and presumably the activity) of ERK1/2, MEK1/2 and CDK2 kinases and that it also markedly increased the activatory phosphorylation of Akt on Ser473. Therefore, multiple pathways transduce mitogenic signals that stimulate centrosome overduplication and clathrin-dependent trafficking is not necessary for effective transduction of the signals leading to centrosome overduplication, as demonstrated by stimulating serum-starved GAK KO cells with EGF. Moreover, when serum-starved GAK KO cells were treated with EGF, there was Plk4 associated with the centrosomes (Fig. 2S), unlike in the serum-starved GAK KO cells. This indicates that clathrin-independent mitogenic signaling is regulating the association of Plk4 with centrosomes. A long residency time of Plk4 on the centrosomes might be related to the overduplication phenotype.

Inhibition of clathrin-dependent trafficking results in centrosome overduplication and growth arrest

Since the phenotype caused by knocking out GAK presumably occurs because loss of this protein disrupts all clathrin trafficking in the cell, we would expect to obtain a similar phenotype by knocking down clathrin. Likewise, since dynamin is required for the budding of clathrin coated pits from the plasma membrane and vesicles from the TGN (40), we would expect to obtain a similar phenotype by inhibiting dynamin using dynasore, a specific pharmacological inhibitor of dynamin (41). It is therefore not surprising that similar to the GAK KO MEFs, both knocking down CHC and treatment of cells with 20 μ M dynasore for 48h resulted in the cessation of DNA synthesis (Fig. 7A) and growth arrest. Histone H3 phosphorylation and cellular DNA content distribution analysis indicated that neither the CHC KD nor the treatment with dynasore caused immediate accumulation of cells in mitosis (Fig. 7B) or any specific cell cycle phase (Fig 7C), just as occurred with the GAK KO MEFs. Also as occurred with the GAK KO MEFs, Western blot analysis revealed that Ser15 phosphorylation of p53 was increased, along with the p21 level in both CHC KD and dynasore-treated cells (Fig. 7D). However, the CDK2 level, phospho-CDK2(Thr160) level and ERK1/2 phosphorylation level were not significantly decreased compared to control cells indicating that mitogenic signaling was generally not disrupted. Cyclin A was diminished, suggesting that the 4N cells are not really G2 cells but have exited the cell cycle in a manner similar to that observed in GAK KO cells. Collectively these results indicate that blocking clathrin-dependent trafficking produced a molecular phenotype similar to the one observed in the GAK KO MEFs.

Since the GAK KO MEFs showed overduplication of centrosomes, we examined whether this phenotype was present in the CHC KD or dynasore- treated cells. Cells transfected with siRNA targeting CHC or treated with 20 μ M dynasore for 48 h were fixed and stained for γ -tubulin and Plk4. In both cases cells with multiple centrosomes positive for Plk4 were observed (Fig. 7E-F). Further population-based studies on centrosome overduplication were conducted using dynasore treatment, since CHC KD efficiency varied between cells and it is not clear what KD efficiency is sufficient for inducing the overduplication phenotype. To establish whether CDK2 and growth factor stimulation are involved in dynasore-induced centrosome overduplication, cells were cultured for 48 h in either medium containing 10% FBS and 20 μ M dynasore or in the same medium supplemented with 20 μ M roscovitine to inhibit CDK2. Alternatively, 10% FBS medium was replaced with low serum medium plus 20 μ M dynasore; 0.5% FBS had to be used here since the dynasore-treated cells were not viable in 0.1% FBS medium. The cells were fixed after 48 h, stained for γ -tubulin and

the centrosomes were counted. Approximately 7% of the control cells exhibited the overduplication phenotype, while in cells treated with dynasore for 48h, the percentage of cells with overduplicated centrosomes increased to 37%. When the dynasore-treated cells were additionally treated with roscovitine or serum-starved, the percentage of cells with overduplicated centrosomes decreased to 11% and 8%, respectively (Fig. 7G). These results show that blocking mitogenic stimulation either by inhibiting CDK2 kinase or reducing mitogenic factors in the medium prevents centrosome overduplication in dynasore-treated cells. Therefore, these data collectively suggest that the phenotypes observed in GAK KO MEFs are caused by inhibiting clathrin-dependent trafficking at the plasma membrane and the TGN.

Discussion

In this report we present the novel finding that inhibition of clathrin-dependent trafficking in MEFs resulted in development of senescence accompanied by centrosome overduplication. Senescence developed because blocking clathrin-dependent trafficking resulted in lysosomal membrane instability and iron leakage, which in turn caused DNA damage. Interestingly, even though the GAK KO MEFs were growth-arrested, they had multiple centrosomes. Moreover, similar phenotypes were observed in MEFs when either clathrin was knocked down using RNAi or when dynamin was inhibited by dynasore. Importantly, when CME was inhibited by knocking down AP2, no DNA damage or senescence was observed although the centrosomes overduplicated. These results indicate that disrupting the CME breaks the link between DNA synthesis and centrosome duplication, allowing multiple rounds of centrosome duplication to occur in growth-arrested cells.

Several laboratories have examined the cell cycle in cells in which clathrin-dependent trafficking has been blocked by treatment with RNAi directed against AP2, clathrin or GAK. There appear to be discrepancies in the literature, with some reports describing fragmented centrosomes in G2/M arrested cells following GAK or CHC knockdown (6, 7, 11, 42) and others find cells arrested in G1 phase with no mention of centrosome overduplication (5, 12). Several of these studies were conducted using HeLa cells, which have an impaired DNA damage response due to the expression of the herpes virus proteins E6 and E7 (43, 44).

In contrast to the above studies, the GAK KO MEFs caused a depletion of mitotic cells, but both 2N and 4N populations were present, with the fraction of 4N cells similar to or lower than in the control MEFs. Our experiments comparing the effects of inhibiting CME by knocking down AP2 and inducing growth arrest by damaging DNA suggest that MEFs require CME-dependent mitogenic stimulation in order to cross the G1/S restriction point and that the low-level DNA damage response primarily activates the G2/M checkpoint. GAK KO MEFs showed a depletion of mitotic cells, unlike the accumulation of mitotic cells observed when GAK or CHC was depleted in HeLa or NRK cells (6, 7). The absence of mitotic cells may be a result of stricter G2/M checkpoint in MEF cells that prevents the cells with damaged DNA from entering mitosis. Alternatively, considering that MEFs, unlike HeLa cells, cannot persist in mitosis for more than a few hours (45, 46), it is possible that the 4N MEFs may have entered mitosis, become arrested at the spindle checkpoint and then eventually escaped mitosis altogether. It may be that both of these alternatives are responsible for the non-G2 4N population in GAK KO MEFs.

A working model of the changes occurring in the various signaling pathways following the disruption of selected trafficking pathways is presented in Fig. 8. In control cells (Fig. 8A) the sum of direct plasma membrane and endocytic signaling provides the composite signal

necessary for DNA replication. Centrosome duplication is synchronized with cell division and as a result cells always contain the proper number of centrosomes.

In contrast, centrosome overduplication and increased Akt phosphorylation as well as growth arrest are observed when endocytosis is inhibited by knocking down AP2, which is only involved in CME, but not in intracellular trafficking (Fig. 8B). Importantly, no DNA damage or senescence is observed in the AP2 KD cells. This suggests that disrupting CME introduces the imbalance in the signaling profile that leads to growth arrest and centrosome overduplication, but is not responsible for DNA damage. On the other hand, when cells are persistently exposed to chemical DNA damaging agents, the cells become senescent, as was observed previously (47). In these cells, trafficking is not disrupted nor is there centrosome overduplication (Fig. 8C). Comparison of the phenotypes caused by AP2 KD or chemical DNA damage clearly shows that the centrosome overduplication is due to a change in signaling resulting from the disruption of CME.

Cells with GAK KO, CHC KD, or inhibition of dynamin, have features of both the AP2KD and the DNA-damage cells in that there is both centrosome overduplication and senescence (Fig. 8D). The former phenotype is apparently caused by alterations in the mitogenic signaling profile due to the inhibition of CME and the latter by concurrent DNA damage. Since cells do not initiate DNA synthesis in the absence of CME (5, 12), it was expected that the GAK KO cells would become quiescent due to the absence of mitogenic signaling. However, knocking out GAK unexpectedly destabilized the lysosomal membrane, which released iron ions that caused DNA damage. The conflicting residual mitogenic signaling and genotoxic stress in the GAK KO cells thus caused senescence rather than quiescence (26, 32).

Collectively our analysis of the signal transduction pathways involved in centrosome overduplication suggest that no single pathway is responsible for this phenomenon, but rather that it is a reflection of a broader signaling profile that is transduced by several pathways that converge on the centrosome. Accordingly, the incidence of centrosome overduplication reflects the level of stimulation received, as exemplified by the intermediate frequency of the overduplication phenotype that occurs in response to EGF treatment of serum-deprived GAK KO cells as compared to cells exposed to complete serum. Our results show that the altered signaling profile that occurs in GAK KO and AP2 KD cells is sufficient to induce centrosome overduplication and growth arrest, while additional exposure to persistent DNA damage is required for senescence.

The connection between trafficking and cell cycle control is frequently overlooked. Cell division and control of centrosome number are important in regard to cellular transformation. Transient disturbances in endocytosis leading to centrosome overduplication and growth arrest, followed by growth resumption may result in the formation of multipolar mitotic spindles, which, in turn, cause inaccurate DNA division and genomic instability. In future studies, the conditional GAK KO system may provide a useful platform to investigate various modes of endosomal signaling by selectively switching off clathrin-dependent pathways without the need for siRNA mediated knockdown or chemical inhibitors with their potential off-target effects.

Materials and Methods

Cells and cell culture

Mouse embryonic fibroblasts were obtained from GAK fl/fl mice as previously described (14). Cells were maintained in DMEM medium containing GlutaMAX (Life Sciences) supplemented with 10% fetal bovine serum (Life Technologies) and penicillin/streptomycin

(Sigma). In order to knock out GAK, cells were infected with Cre-encoding adenovirus (Vector Biolabs, Philadelphia, PA) at the MOI ratio of 100:1, with 6 μ g/ml polybrene (Sigma), replated 3 days later and at the times indicated used for experiments. In clathrin knockdown experiments the cells over the course of 6 days were transfected twice with siRNA (20 nM) using Lipofectamine RNAiMAX (Life Technologies) according to manufacturer's instructions. In AP2 knockdown experiments the cells were infected twice, 48 h apart, with lentiviruses encoding shRNA directed against α -adaptin (AP2A1 and AP2A2, TRC clones TRCN0000277543 and TRCN0000238173), obtained from Sigma. Roscovitine, UO126, SB203580 (LC Laboratories), Akt inhibitor VIII, dynasore (EMD Millipore), hydroxyurea, desferroxamine (Sigma) and KU55399 (Tocris Biosciences) were used at concentrations and for times indicated in text and figure legends.

Cell growth, DNA replication and flow cytometry

Cell growth and multiplication were assayed by methylene blue method as published previously (17). Senescence was detected by beta-galactosidase staining as published previously (19). DNA synthesis was assayed with 5-ethynyl-2'-deoxyuridine (EdU) method, an alternative to BrdU, using the kit from Life Technologies. The cells were stained in suspension or on coverslips and the cells positive for EdU were counted using flow cytometry or confocal microscopy, respectively. Phosphorylated histone H3 (Ser28) was stained to label mitotic cells; the cells were then counterstained with propidium iodide and analyzed by flow cytometry using FACSCalibur instrument.

In vitro DNA replication assay

Cytosolic fractions were prepared from S-phase-synchronized control MEFs and non-synchronized GAK KO cells and nuclei were prepared from non-synchronized control MEFs and GAK KO MEFs by cell swelling and disruption in a hypotonic buffer as described (20). The DNA synthesis reaction and fluorescent labeling were performed as described (48) using biotin-labeled dUTP (Roche Applied Science) and FITC-streptavidin (Sigma).

Immunofluorescent staining and confocal microscopy

For immunofluorescent staining the cells were grown on coverslips and fixed in 4% paraformaldehyde in PBS. Primary and secondary antibodies were diluted in 3% BSA/0.1% saponin/PBS. After final washing the coverslips were mounted in SlowFade Gold (Life Technologies) and imaged under Zeiss LSM510 confocal microscope. Any adjustments of brightness or contrast introduced to enhance feature visibility were linear and such as not to obscure any image features. In EdU incorporation and centrosome-counting experiments at least three independent experiments were performed with the aggregate number of counted cells $n > 300$. Repeated measures ANOVA followed by Bonferroni's or Tukey's (as appropriate) multiple comparison test was performed using GraphPad Prism 5.

For fluorescence recovery after photobleaching (FRAP) experiments control cells and GAK KO cells were seeded in LabTek chambers on day 3 post-infection. The following day the cells were transfected with a plasmid encoding GFP-LCa (clathrin light chain). On day 6 post-infection the cells were imaged. Following the bleaching recovery was monitored for 5 minutes by which time fluorescence intensity plateaued.

Antibodies

The following antibodies were used for Western blotting, immunoprecipitation and immunofluorescent staining: GAK (homemade); clathrin heavy chain, p19ARF, S28-phospho-H3, α -tubulin and centrin 1 from Abcam; GAPDH, CDK2, Cyclin E, Cyclin A,

p53, p21 and p16 from Santa Cruz; p27/Kip and α -adaptin from BD Transduction Labs, Plk4, S1981-phospho-ATM, T202/Y204-phospho-ERK, S217/S221-phospho-MEK, S473-phospho-Akt, T160-phospho-CDK2 and S15-phospho-p53 from Cell Signaling; ERK1/2 and Akt from Enzo Life Sciences; MEK1+2 from GeneTex; γ -tubulin from Sigma.

CDK2 coimmunoprecipitation and kinase assay

MEF cells were lysed in PBS supplemented with 0.1% NP40, 0.1% Triton X-100 and EDTA-free protease and phosphatase inhibitor cocktail (Thermo Scientific). Cleared lysates were incubated overnight at 4°C with protein G beads (Sigma) coated with anti-CDK2 antibody. 2 μ g of antibody and lysate containing 0.5 mg total protein were used per immunoprecipitation reaction. The beads were then washed 5 times in the co-IP buffer and suspended in kinase reaction buffer (25 mM Tris pH 7.5, 10 mM MgCl₂, 2 mM EGTA, 2 mM DTT, 0.2 mM ATP) pre-warmed to 30°C and containing 5 μ Ci of [³²P]ATP (Perkin Elmer) and 3 μ g of histone H1⁰ (New England Biolabs) per reaction. The beads were resuspended every 5 min and after 30 minutes the reaction was stopped by the addition of SDS sample buffer and heating for 5 min at 95°C. The samples were then resolved by SDS-PAGE, the gel was dried and exposed to a screen (Kodak) that was read using Fuji fluorescence scanner.

The cells were incubated for 15 min with 2 μ g/ml acridine orange (Sigma) dissolved in culture medium. The medium was then replaced and the cells were imaged using 488 nm laser illumination set to such intensity as to induce complete lysosome bursting in control cells after approximately 80 frames. 560LP filter was used for emission. GAK KO cells were imaged under these same settings and the number of centrosomes was quantified using ImageJ software (NIH). The experiment was performed 3 times, with at least 10 cells imaged per condition.

Supplementary Material

Refer to Web version on PubMed Central for supplementary material.

Acknowledgments

Maciej Olszewski was supported by Foundation for Polish Science grant “Kolumb”

References

1. Hoeller D, Volarevic S, Dikic I. Compartmentalization of growth factor receptor signalling. *Curr Opin Cell Biol.* 2005; 17(2):107–111. [PubMed: 15780584]
2. Polo S, Di Fiore PP. Endocytosis conducts the cell signaling orchestra. *Cell.* 2006; 124(5):897–900. [PubMed: 16530038]
3. Sorkin A, von Zastrow M. Endocytosis and signalling: intertwining molecular networks. *Nat Rev Mol Cell Biol.* 2009; 10(9):609–622. [PubMed: 19696798]
4. Sadowski L, Pilecka I, Miaczynska M. Signaling from endosomes: location makes a difference. *Exp Cell Res.* 2009; 315(9):1601–1609. [PubMed: 18930045]
5. Sigismund S, Argenzio E, Tosoni D, Cavallaro E, Polo S, Di Fiore PP. Clathrin-mediated internalization is essential for sustained EGFR signaling but dispensable for degradation. *Dev Cell.* 2008; 15(2):209–219. [PubMed: 18694561]
6. Royle SJ, Bright NA, Lagnado L. Clathrin is required for the function of the mitotic spindle. *Nature.* 2005; 434(7037):1152–1157. [PubMed: 15858577]
7. Shimizu H, Nagamori I, Yabuta N, Nojima H. GAK, a regulator of clathrin-mediated membrane traffic, also controls centrosome integrity and chromosome congression. *J Cell Sci.* 2009; 122(Pt 17):3145–3152. [PubMed: 19654208]

8. Eisenberg E, Greene LE. Multiple roles of auxilin and hsc70 in clathrin-mediated endocytosis. *Traffic*. 2007; 8(6):640–646. [PubMed: 17488288]
9. Greener T, Zhao X, Nojima H, Eisenberg E, Greene LE. Role of cyclin G-associated kinase in uncoating clathrin-coated vesicles from non-neuronal cells. *J Biol Chem*. 2000; 275(2):1365–1370. [PubMed: 10625686]
10. Lee DW, Zhao X, Zhang F, Eisenberg E, Greene LE. Depletion of GAK/auxilin 2 inhibits receptor-mediated endocytosis and recruitment of both clathrin and clathrin adaptors. *J Cell Sci*. 2005; 118(Pt 18):4311–4321. [PubMed: 16155256]
11. Foraker AB, Camus SM, Evans TM, Majeed SR, Chen CY, Taner SB, Correa IR Jr, Doxsey SJ, Brodsky FM. Clathrin promotes centrosome integrity in early mitosis through stabilization of centrosomal ch-TOG. *J Cell Biol*. 2012; 198(4):591–605. [PubMed: 22891263]
12. Sousa LP, Lax I, Shen H, Ferguson SM, Camilli PD, Schlessinger J. Suppression of EGFR endocytosis by dynamin depletion reveals that EGFR signaling occurs primarily at the plasma membrane. *Proc Natl Acad Sci U S A*. 2012; 109(12):4419–4424. [PubMed: 22371560]
13. Sadowski L, Jastrzebski K, Kalaidzidis Y, Heldin CH, Hellberg C, Miaczynska M. Dynamin inhibitors impair endocytosis and mitogenic signaling of PDGF. *Traffic*. 2013; 14(6):725–736. [PubMed: 23425318]
14. Lee DW, Zhao X, Yim YI, Eisenberg E, Greene LE. Essential role of cyclin-G-associated kinase (Auxilin-2) in developing and mature mice. *Molecular biology of the cell*. 2008; 19(7):2766–2776. [PubMed: 18434600]
15. Lee DW, Wu X, Eisenberg E, Greene LE. Recruitment dynamics of GAK and auxilin to clathrin-coated pits during endocytosis. *J Cell Sci*. 2006; 119(Pt 17):3502–3512. [PubMed: 16895969]
16. Kametaka S, Moriyama K, Burgos PV, Eisenberg E, Greene LE, Mattera R, Bonifacino JS. Canonical interaction of cyclin G associated kinase with adaptor protein 1 regulates lysosomal enzyme sorting. *Mol Biol Cell*. 2007; 18(8):2991–3001. [PubMed: 17538018]
17. Pelletier B, Dhainaut F, Pauly A, Zahnd JP. Evaluation of growth rate in adhering cell cultures using a simple colorimetric method. *J Biochem Biophys Methods*. 1988; 16(1):63–73. [PubMed: 2456322]
18. Dimri GP, Lee X, Basile G, Acosta M, Scott G, Roskelley C, Medrano EE, Linskens M, Rubelj I, Pereira-Smith O, et al. A biomarker that identifies senescent human cells in culture and in aging skin in vivo. *Proc Natl Acad Sci U S A*. 1995; 92(20):9363–9367. [PubMed: 7568133]
19. Debacq-Chainiaux F, Erusalimsky JD, Campisi J, Toussaint O. Protocols to detect senescence-associated beta-galactosidase activity, a biomarker of senescent cells in culture and in vivo. *Nat Protoc*. 2009; 4(12):1798–1806. [PubMed: 20010931]
20. Krude T, Jackman M, Pines J, Laskey RA. Cyclin/Cdk-dependent initiation of DNA replication in a human cell-free system. *Cell*. 1997; 88(1):109–119. [PubMed: 9019396]
21. Prosser SL, Straatman KR, Fry AM. Molecular dissection of the centrosome overduplication pathway in S-phase-arrested cells. *Mol Cell Biol*. 2009; 29(7):1760–1773. [PubMed: 19139275]
22. Habedanck R, Stierhof YD, Wilkinson CJ, Nigg EA. The Polo kinase Plk4 functions in centriole duplication. *Nat Cell Biol*. 2005; 7(11):1140–1146. [PubMed: 16244668]
23. Kleylein-Sohn J, Westendorf J, Le Clech M, Habedanck R, Stierhof YD, Nigg EA. Plk4-induced centriole biogenesis in human cells. *Dev Cell*. 2007; 13(2):190–202. [PubMed: 17681131]
24. Rogers GC, Rusan NM, Roberts DM, Peifer M, Rogers SL. The SCF Slimb ubiquitin ligase regulates Plk4/Sak levels to block centriole reduplication. *J Cell Biol*. 2009; 184(2):225–239. [PubMed: 19171756]
25. Campisi J, d'Adda di Fagagna F. Cellular senescence: when bad things happen to good cells. *Nat Rev Mol Cell Biol*. 2007; 8(9):729–740. [PubMed: 17667954]
26. Demidenko ZN, Blagosklonny MV. Growth stimulation leads to cellular senescence when the cell cycle is blocked. *Cell Cycle*. 2008; 7(21):3355–3361. [PubMed: 18948731]
27. Dulic V, Drullinger LF, Lees E, Reed SI, Stein GH. Altered regulation of G1 cyclins in senescent human diploid fibroblasts: accumulation of inactive cyclin E-Cdk2 and cyclin D1-Cdk2 complexes. *Proc Natl Acad Sci U S A*. 1993; 90(23):11034–11038. [PubMed: 8248208]

28. Hanashiro K, Kanai M, Geng Y, Sicinski P, Fukasawa K. Roles of cyclins A and E in induction of centrosome amplification in p53-compromised cells. *Oncogene*. 2008; 27(40):5288–5302. [PubMed: 18490919]
29. Stein GH, Drullinger LF, Soulard A, Dulic V. Differential roles for cyclin-dependent kinase inhibitors p21 and p16 in the mechanisms of senescence and differentiation in human fibroblasts. *Mol Cell Biol*. 1999; 19(3):2109–2117. [PubMed: 10022898]
30. Campaner S, Doni M, Hydbring P, Verrecchia A, Bianchi L, Sardella D, Schleker T, Perna D, Tronnorsjo S, Murga M, Fernandez-Capetillo O, Barbacid M, Larsson LG, Amati B. Cdk2 suppresses cellular senescence induced by the c-myc oncogene. *Nat Cell Biol*. 2010; 12(1):54–59. sup pp 51-14. [PubMed: 20010815]
31. Freedman DA, Folkman J. CDK2 translational down-regulation during endothelial senescence. *Exp Cell Res*. 2005; 307(1):118–130. [PubMed: 15922732]
32. Leontieva OV, Blagosklonny MV. DNA damaging agents and p53 do not cause senescence in quiescent cells, while consecutive re-activation of mTOR is associated with conversion to senescence. *Aging (Albany NY)*. 2010; 2(12):924–935. [PubMed: 21212465]
33. Bakkenist CJ, Kastan MB. DNA damage activates ATM through intermolecular autophosphorylation and dimer dissociation. *Nature*. 2003; 421(6922):499–506. [PubMed: 12556884]
34. Al Rashid ST, Dellaire G, Cuddihy A, Jalali F, Vaid M, Coackley C, Folkard M, Xu Y, Chen BP, Chen DJ, Lilge L, Prise KM, Bazett Jones DP, Bristow RG. Evidence for the direct binding of phosphorylated p53 to sites of DNA breaks in vivo. *Cancer Res*. 2005; 65(23):10810–10821. [PubMed: 16322227]
35. Kruszewski M, Iwanenko T. Labile iron pool correlates with iron content in the nucleus and the formation of oxidative DNA damage in mouse lymphoma L5178Y cell lines. *Acta Biochim Pol*. 2003; 50(1):211–215. [PubMed: 12673362]
36. Kakhlon O, Cabantchik ZI. The labile iron pool: characterization, measurement, and participation in cellular processes(1). *Free Radic Biol Med*. 2002; 33(8):1037–1046. [PubMed: 12374615]
37. Kurz T, Leake A, von Zglinicki T, Brunk UT. Lysosomal redox-active iron is important for oxidative stress-induced DNA damage. *Ann N Y Acad Sci*. 2004; 1019:285–288. [PubMed: 15247030]
38. Kurz T, Leake A, Von Zglinicki T, Brunk UT. Relocalized redox-active lysosomal iron is an important mediator of oxidative-stress-induced DNA damage. *Biochem J*. 2004; 378(Pt 3):1039–1045. [PubMed: 14670081]
39. Kirkegaard T, Roth AG, Petersen NH, Mahalka AK, Olsen OD, Moilanen I, Zylicz A, Knudsen J, Sandhoff K, Arenz C, Kinnunen PK, Nylandsted J, Jaattela M. Hsp70 stabilizes lysosomes and reverts Niemann-Pick disease-associated lysosomal pathology. *Nature*. 2010; 463(7280):549–553. [PubMed: 20111001]
40. Cao H, Thompson HM, Krueger EW, McNiven MA. Disruption of Golgi structure and function in mammalian cells expressing a mutant dynamin. *J Cell Sci*. 2000; 113(Pt 11):1993–2002. [PubMed: 10806110]
41. Macia E, Ehrlich M, Massol R, Boucrot E, Brunner C, Kirchhausen T. Dynasore, a cell-permeable inhibitor of dynamin. *Dev Cell*. 2006; 10(6):839–850. [PubMed: 16740485]
42. Tanenbaum ME, Vallenius T, Geers EF, Greene L, Makela TP, Medema RH. Cyclin G-associated kinase promotes microtubule outgrowth from chromosomes during spindle assembly. *Chromosoma*. 2010; 119(4):415–424. [PubMed: 20237935]
43. Kessis TD, Slebos RJ, Nelson WG, Kastan MB, Plunkett BS, Han SM, Lorincz AT, Hedrick L, Cho KR. Human papillomavirus 16 E6 expression disrupts the p53-mediated cellular response to DNA damage. *Proc Natl Acad Sci U S A*. 1993; 90(9):3988–3992. [PubMed: 8387205]
44. Funk JO, Waga S, Harry JB, Espling E, Stillman B, Galloway DA. Inhibition of CDK activity and PCNA-dependent DNA replication by p21 is blocked by interaction with the HPV-16 E7 oncoprotein. *Genes & development*. 1997; 11(16):2090–2100. [PubMed: 9284048]
45. Lanni JS, Jacks T. Characterization of the p53-dependent postmitotic checkpoint following spindle disruption. *Mol Cell Biol*. 1998; 18(2):1055–1064. [PubMed: 9448003]

46. Margolis RL, Lohez OD, Andreassen PR. G1 tetraploidy checkpoint and the suppression of tumorigenesis. *J Cell Biochem.* 2003; 88(4):673–683. [PubMed: 12577301]
47. McKenna E, Traganos F, Zhao H, Darzynkiewicz Z. Persistent DNA damage caused by low levels of mitomycin C induces irreversible cell senescence. *Cell Cycle.* 2012; 11(16):3132–3140. [PubMed: 22871735]
48. Krude T. Chromatin assembly factor 1 (CAF-1) colocalizes with replication foci in HeLa cell nuclei. *Experimental cell research.* 1995; 220(2):304–311. [PubMed: 7556438]

Synopsis

Knocking out GAK, a HSC70 cochaperone essential for chaperoning clathrin causes senescence and centrosome overduplication. Disruption of clathrin-mediated endocytosis leads to alterations in mitogenic signaling profile which causes growth arrest and centrosome overduplication. Concurrent disruption of intracellular clathrin-dependent trafficking results in lysosomal membrane destabilization causing iron leakage that leads to DNA damage. Prolonged exposure to DNA damage in the presence of mitogenic stimulation leads to the development of senescence accompanied by centrosome overduplication.

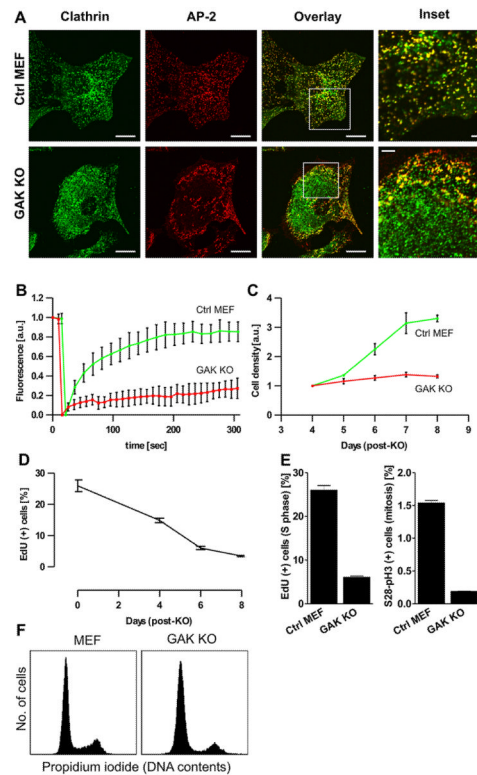


Fig. 1. GAK depletion causes disruption of clathrin function and growth arrest.

MEFs were infected with AdCre and plated 3 days post-infection. **(A)** Immunofluorescent staining for clathrin heavy chain (green) and AP-2 (red). Clathrin distribution is changed and colocalization with AP-2 largely abolished. Scale bars represent 20 μm in low magnification images and 5 μm in high magnification inserts **(B)** FRAP analysis of GFP-clathrin exchange in clathrin-coated pits. Only a small fraction of bleached GFP-clathrin is exchanged in GAK KO cells when compared to control cells. **(C)** GAK KO cells cease to grow. Cell number was assayed by methylene blue staining. **(D)** GAK KO cells do not replicate DNA. Cells were labeled with 20 μM EdU for 1 h, stained for EdU and analyzed by FACS. **(E, F)** GAK KO cells do not accumulate in G2 or mitosis. Control and GAK KO cells 6 days after knockout were labeled with 20 μM EdU for 1 h and stained for EdU and phospho-Ser28-H3 **(E)** or stained with propidium iodide **(F)** and analyzed by FACS. Error bars denote s.e.m.

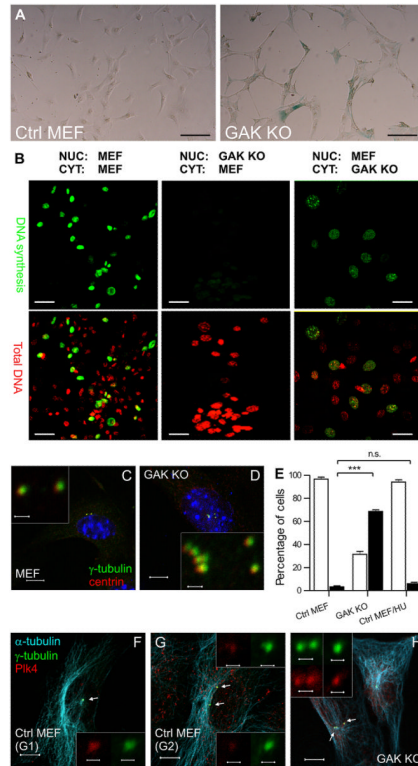


Fig. 2. GAK KO causes senescence and centrosome overduplication.

(A) GAK KO cells were fixed 10 d after AdCre infection. Cells were stained for β -galactosidase, a marker of senescence. Scale bars represent 100 μ m. (B) The nuclei and cytosol isolated from control and GAK KO cells were tested in vitro for proliferative capacity. Newly synthesized DNA and total DNA are shown in green and red, respectively. Scale bars represent 50 μ m. (C, D) GAK KO cells overduplicate centrosomes. Cells were stained for γ -tubulin (green) and centrin (red). Multiple centrosomes positive for both markers are visible in GAK KO cell. Scale bars represent 10 μ m in low magnification images and 1 μ m in high magnification inserts. (E) Quantification of cells with overduplicated centrosomes (more than 2 per cell) in control, GAK KO and 2 mM hydroxyurea-treated cells. Open and closed bars denote cells containing 1-2 or >2 centrosomes, respectively. $n > 300$, *** and n.s. indicate $p < 0.001$ and $p > 0.05$, respectively. Error bars denote s.e.m. (F-H) MEF cells grown on coverslips were stained for Plk4 and γ -tubulin. In G1 cells (F) (1 centrosome/cell) but not in S/G2 cells (G) (2 centrosomes/cell) Plk4 is observed at the centrosome. (H) GAK KO MEF cells grown on coverslips were fixed 6 d after AdCre infection and stained for Plk4 and γ -tubulin. Scale bars represent 10 μ m in low magnification images and 1 μ m in high magnification inserts.

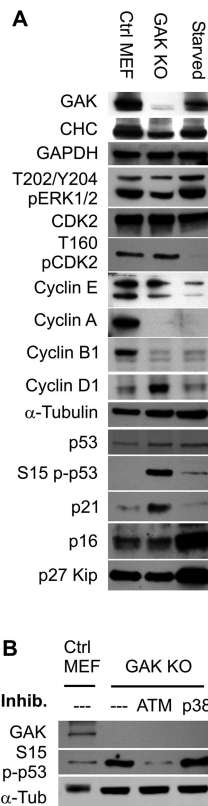


Fig. 3. Molecular phenotype of GAK KO cells is consistent with senescence.

(A) Control and AdCre-infected MEFs were harvested after 6 days of culture in 10% FBS medium. Alternatively control MEFs were cultured in 0.1 % FBS medium for 48 h to induce quiescent phenotype. Lysates were analyzed by Western blotting (B) GAK KO cells were treated with 20 μ M KU55933 (ATM inhibitor) or 8 μ M SB203580 (p38 inhibitor) for 24 h, beginning at day 6 post-KO. Lysates were analyzed by Western blotting.

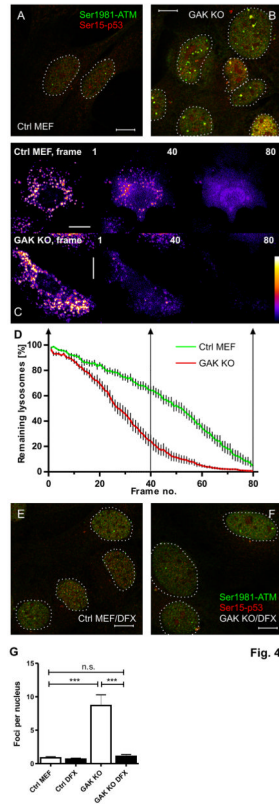


Fig. 4. Lysosomal membrane instability in GAK KO cells leads to iron leak and DNA damage. (A-B) Control and GAK KO MEFs (6 d after AdCre infection) were stained for phospho-Ser1981-ATM (green) and phospho-Ser15-p53 (red). Foci visible in GAK KO nuclei represent DNA strand breaks. Scale bar represents 10 μ m. (C-D) Lysosomal membrane stability was assayed by acridine orange-mediated photodamage method. Control and GAK KO cells were incubated for 15 min with 2 μ g/ml acridine orange and imaged under low-level 488 nm illumination. (C) Comparison of light-induced photodamage in control and GAK KO cells in frames 1, 40 and 80 of the sequence. Scale bars represent 20 μ m (D) Decrease in lysosome number during imaging due to light-induced photodamage. Lysosomes were counted in at least 10 cells per condition. Error bars represent s.e.m. (E-F) Lysosome-derived iron causes DNA damage in GAK KO cells. Control and GAK KO cells were incubated with 0.2 mM desferrioxamine (DFX) for 12 h and stained for phospho-Ser15-p53 (red) and phospho-Ser1981-ATM (green). Treatment of GAK KO cells with DFX decreases the number of DNA breaks. Scale bar represents 10 μ m. (G) Quantification of the nuclear foci shown in (A-B) and (E-F). $n > 100$, *** $p < 0.001$, n.s $p > 0.05$, error bars represent s.e.m.

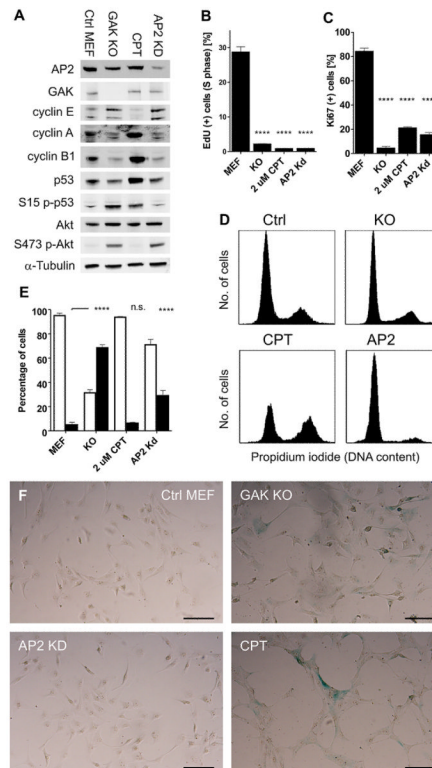


Fig. 5. Disrupted endocytosis causes centrosome overduplication while concomitant persistent DNA damage leads to senescence.

(A-E) Cells were treated as follows: non-treated (control), GAK KO (6 d), camptothecin (2 μ M, 48 h) and AP2 KD (6 d) (A) Cells were lysed and the lysates were analyzed by Western blotting. (B) Cells were labeled with 20 μ M EdU for 1 h, stained for EdU and analyzed by FACS. (C) Cells grown on coverslips were stained for Ki67 nuclei positive for Ki67 were counted. (D) Cells were stained with propidium iodide and analyzed by flow cytometry. (E) Cells grown on coverslips were stained for γ -tubulin and centrosomes were counted. Open and closed bars denote cells containing 1-2 or >2 centrosomes, respectively. (F) GAK KO cells were seeded on coverslips on day 4 post-AdCre infection. AP2 KD cells were seeded on coverslips 4 days after the first and 2 days after the second lentiviral infection. Both types of cells were fixed 10 days after initial infection. CPT-treated cells were exposed to 2 μ M camptothecin for 3 h daily for 6 days and then fixed. All cells were stained for β -galactosidase. Scale bars represent 100 μ m.

In all panels $n > 300$, **** and n.s. indicate $p < 0.0001$ and $p > 0.05$, respectively. Error bars denote s.e.m.

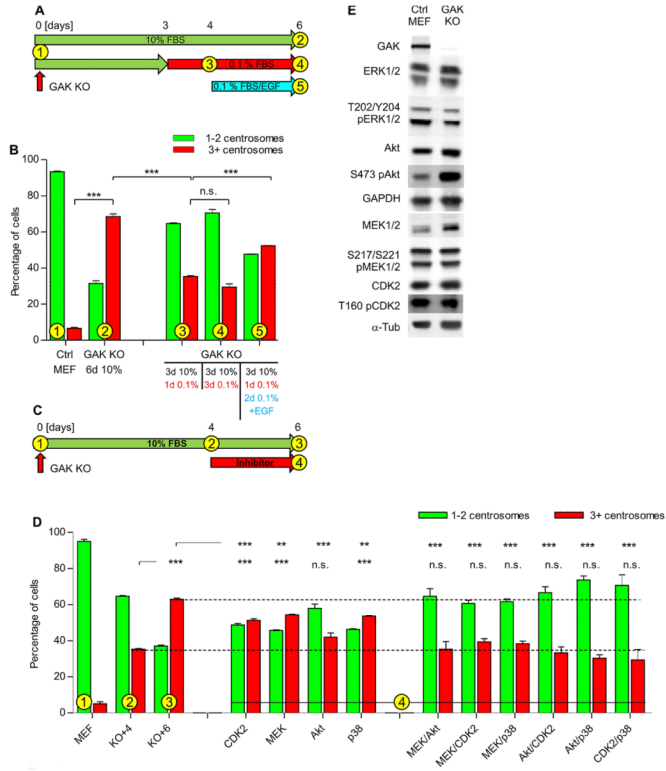


Fig. 6. Growth factor signaling required for centrosome overduplication in GAK KO cells is transduced by multiple kinases (A,B)

MEFs were infected with AdCre, replated on coverslips on day 3 post-infection and culture media were replaced according to the scheme presented in (A). The cells were fixed, stained for γ -tubulin and the centrosomes were counted under the fluorescence microscope. $n > 300$, *** $p < 0.001$, n.s. $p > 0.05$ (C,D) Cells were cultured according to the scheme presented in (C); culture media were supplemented with CDK2, MEK, Akt and p38 inhibitors: roscovitine (20 μ M), UO126 (10 μ M), AktVIII (10 μ M) and SB203580 (4 μ M), respectively, or combinations thereof. The cells were fixed, stained for γ -tubulin and the centrosomes were counted under fluorescence microscope. (E) Control and AdCre-infected MEFs were harvested after 6 days of culture in 10% FBS medium. Lysates were analyzed by Western blotting.

In all panels error bars denote s.e.m. $n > 300$, *** $p < 0.001$, ** $p < 0.01$, n.s. $p > 0.05$

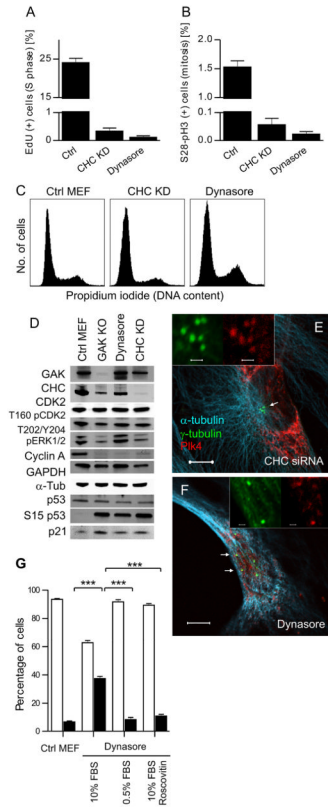


Fig. 7. Inhibition of clathrin-dependent trafficking results in centrosome overduplication and growth arrest (A-C)

MEF cells were transfected with CHC siRNA or treated for 48 h with 20 μ M dynasore. The cells were subsequently labeled with 20 μ M EdU for 1 h and stained for EdU, phospho-Ser28-H3 or with propidium iodide. Cells were analyzed by FACS, and (A) percentage of cells positive for EdU or (B) phospho-Ser28-H3 is shown. (C) DNA content distribution was analyzed by propidium iodide staining followed by FACS. (D) Western blot analysis of control, GAK KO, dynasore-treated and CHC KD cells. (E, F) CHC KD and dynasore-treated cells were grown on coverslips in medium containing 10% FBS and stained for Plk4, α -tubulin and γ -tubulin. Representative cells are presented, showing multiple centrosomes, positive for Plk4. Scale bars represent 10 μ m in low magnification images and 1 μ m in high magnification inserts. (G) MEF cells grown on coverslips were cultured for 48 h in medium containing 10% FBS, 10% FBS and 20 μ M dynasore, 0.5% FBS and 20 μ M dynasore or 10% FBS, 20 μ M dynasore and 20 μ M roscovitine. Cells were stained for γ -tubulin and centrosomes were counted under fluorescence microscope. Open and closed bars denote cells containing 1-2 or >2 centrosomes, respectively. n>300, *** p<0.001. In (A) and (F) error bars denote s.e.m.

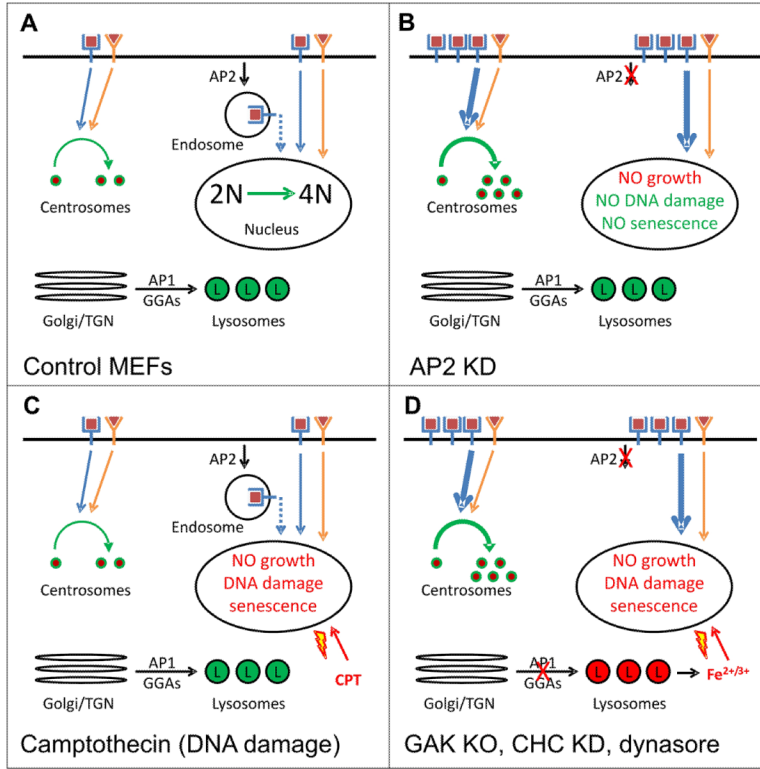


Fig. 8. (A-D) Working model depicting signaling and trafficking in (A) control MEFs and changes in signaling pathways leading to centrosome overduplication and/or senescence in (B) cells in which specifically clathrin-dependent endocytosis was disrupted, (C) cells in which DNA damage was induced by camptothecin treatment, and (D) cells in which all clathrin-dependent trafficking was disrupted (GAK KO, CHC KD and dynasore-treated cells).